entropy

MDPI

Article

The Generalized Euler Characteristics of the Graphs Split at Vertices

Omer Farooq *, Michał Ławniczak *, Afshin Akhshani, Szymon Bauch and Leszek Sirko *

Institute of Physics, Polish Academy of Sciences, Aleja Lotników 32/46, 02-668 Warsaw, Poland; akhshani@ifpan.edu.pl (A.A.); bauch@ifpan.edu.pl (S.B.)

* Correspondence: omer.farooq@ifpan.edu.pl (O.F.); lawni@ifpan.edu.pl (M.Ł.); sirko@ifpan.edu.pl (L.S.)

Abstract: We show that there is a relationship between the generalized Euler characteristic $\mathcal{E}_o(|V_{D_o}|)$ of the original graph that was split at vertices into two disconnected subgraphs $i = 1, 2$ and their generalized Euler characteristics $\mathcal{E}_i(|V_{D_i}|)$. Here, $|V_{D_o}|$ and $|V_{D_i}|$ denote the numbers of vertices with the Dirichlet boundary conditions in the graphs. The theoretical results are experimentally verified using microwave networks that simulate quantum graphs. We demonstrate that the evaluation of the generalized Euler characteristics $\mathcal{E}_o(|V_{D_o}|)$ and $\mathcal{E}_i(|V_{D_i}|)$ allow us to determine the number of vertices where the two subgraphs were initially connected.

Keywords: quantum graphs; microwave networks; Euler characteristic; Neumann and Dirichlet boundary conditions

check for updates

Citation: Farooq, O.; Ławniczak, M.; Akhshani, A.; Bauch, S.; Sirko, L. The Generalized Euler Characteristics of the Graphs Split at Vertices. *Entropy* **2022**, *24*, 387. https://doi.org/10.3390/e24030387

Academic Editor: Adam Gadomski

Received: 2 February 2022
Accepted: 8 March 2022
Published: 9 March 2022

1. Introduction

The concept of graphs was already introduced in the XVIII century by Leonhard Euler [1]. Two hundred years later, Linus Pauling [2] considered quantum graphs in order to describe the motion of quantum particles in a physical network. The models of quantum graphs were widely used to investigate many physical systems, e.g., quantum wires [3], mesoscopic quantum systems [4,5], a topological edge invariant [6], and the photon number statistics of coherent light [7]. Broad applications of graphs and networks mean that the theory of quantum graphs has been a subject of extensive research [8–14].

We will consider a metric graph $\Gamma = (V, E)$, which consists of v vertices, $v \in V$, connected by e edges, $e \in E$. The edges e are intervals of the length l_e on the real line $\mathbb{R}$. The metric graph becomes quantum when we equip it with the free Schrödinger operator. In our case, this is the one-dimensional Laplace operator, which equals $L(\Gamma) = -\frac{d^2}{dx_e^2}$ on each of the edges $e \in E$ of the graph Γ. The self-adjoint Laplace operator $L(\Gamma)$ has a discrete and non-negative spectrum [12].

A signal inside a graph moves along the edges, and at each vertex $v \in V$ it splits and enters all edges adjacent to v. If the signal enters the vertex v along the edge e' and leaves it along the edge e, then the ratio of amplitudes of entering and leaving signals is given by the vertex scattering matrix, which depends on the vertex boundary condition. We will consider two types of vertex boundary conditions. The standard boundary conditions are called also Neumann boundary conditions, for which the eigenfunctions are continuous at vertices and the sums of their oriented derivatives at vertices are zero. The vertex scattering matrix corresponding to the Neumann boundary conditions [15] is given by

$$ {}^{N}\sigma^{(v)}_{e,e'} = \frac{2}{d_v} - \delta_{e,e'}, \tag{1} $$

where d_v is the degree of the vertex v, i.e., the number of edges incident to the vertex v, and $\delta_{e,e'}$ is the Kronecker delta. The vertices with the Neumann boundary conditions will be denoted as v_N.

For the Dirichlet boundary condition, an eigenfunction at the vertex takes the value zero, which leads to the vertex scattering matrix [15,16]

$$^{D}\sigma^{(v)}_{e,e'} = -\delta_{e,e'}. \tag{2}$$

One should point out that the Dirichlet boundary conditions are imposed only at degree one vertices and higher-degree Dirichlet vertices should be treated as separate degree one Dirichlet vertices. The vertices with the Dirichlet boundary conditions will be denoted as v_D. Different types of the boundary conditions, including the Neumann and Dirichlet ones for higher-dimensional systems such as grains, are comprehensively described in Refs. [17,18].

The total number of vertices $|V|$ in a general graph, consisting of both Neumann and Dirichlet boundary conditions, is defined by $|V| = |V_N| + |V_D|$, where $|V_N|$ and $|V_D|$ denote the number of vertices with Neumann and Dirichlet boundary conditions, respectively.

One of the most important characteristics of metric graphs $\Gamma = (V, E)$ with the standard boundary conditions ($|V_D| = 0$) is the Euler characteristic

$$\chi = |V| - |E|\,, \tag{3}$$

where $|V|$ and $|E|$ denote the number of vertices and edges of the graph. It is a purely topological quantity; however, it has been shown in [19–22] that it can also be defined by the graph and microwave network spectra. The formula describing the generalized Euler characteristic $\mathcal{E}$ [22,23], which is also applicable for graphs and networks with the Dirichlet boundary conditions, will be discussed later.

In the experimental investigation of properties of quantum graphs, we used microwave networks simulating quantum graphs [16,24–29]. The emulation of quantum graphs by microwave networks is possible because of the formal analogy of the one-dimensional Schrödinger equation describing quantum graphs and the telegrapher's equation for microwave networks [24,26]. Microwave networks are the only ones that allow for the experimental simulation of quantum systems with all three types of symmetry within the framework of the random matrix theory (RMT): Gaussian orthogonal ensemble (GOE)—systems with preserved time reversal symmetry (TRS) [16,21,24,25,27,30–32], Gaussian unitary ensemble (GUE)—systems with broken TRS [24,28,33–36], and Gaussian symplectic ensemble (GSE)—systems with TRS and half-spin [37]. The other model systems, which are not as versatile as microwave networks, but are often used in simulations of complex quantum systems, are flat microwave billiards [38–54], and exited atoms in strong microwave fields [55–67].

In this article, we will analyze the splitting of a quantum graph (network) into two disconnected subgraphs (subnetworks). Using a currently introduced spectral invariant—the generalized Euler characteristic $\mathcal{E}$ [22]—we determine the number $|V_c|$ of common vertices where the two subgraphs were initially connected. The application of the generalized Euler characteristic $\mathcal{E}$ for this purpose stems from the fact that it can be evaluated without knowing the topologies of quantum graphs (networks), using small or moderate numbers of their lowest eigenenergies (resonances). The theoretical results are numerically verified and confirmed experimentally using the spectra of microwave networks simulating quantum graphs.

2. Theoretical Outline

2.1. The Generalized EULER Characteristic

In Refs. [21,22], the formulas for the Euler characteristic for graphs with the standard boundary conditions at the vertices and with the mixed ones, standard and Dirichlet boundary conditions at vertices, were derived. In the case of the standard boundary conditions,

$$\chi = 2 + 8\pi^2 \sum_{\substack{k_n \in \Sigma(L^{\mathrm{st}}(\Gamma)) \\ k_n \neq 0}} \frac{\sin(k_n/t)}{(k_n/t)\left((2\pi)^2 - (k_n/t)^2\right)}|_{t \geq t_0}, \tag{4}$$

where $\Sigma(L^{\mathrm{st}}(\Gamma))$ denotes the spectrum of the Laplacian $L^{\mathrm{st}}(\Gamma)$ with the standard vertex conditions, taken in the square root scale, i.e., the numbers k_n are the square roots of the eigenenergies λ_n and t is a scaling parameter [19–21] with $t_0 = \frac{1}{2l_{min}}$, where l_{min} is the length of the shortest edge of the graph. The above formula is equivalent to Equation (3); however, instead of using topological information about graphs or networks, such as the number of vertices $|V|$ and edges $|E|$, it requires a certain number of the lowest eigenenergies (resonances) of graphs or networks.

For graphs and networks with the mixed boundary conditions, namely the standard and Dirichlet ones ($|V_D| \neq 0$), the generalized Euler characteristic can be expressed by the following formula:

$$\chi_G := \chi - |V_D| = 8\pi^2 \sum_{k_n \in \Sigma(L^{\mathrm{st,D}}(\Gamma))} \frac{\sin(k_n/t)}{(k_n/t)\left((2\pi)^2 - (k_n/t)^2\right)}|_{t \geq t_0}. \tag{5}$$

In Equation (5), the spectrum of the Laplacian $L^{\mathrm{st,D}}(\Gamma)$ with the standard and Dirichlet vertex conditions is denoted by $\Sigma(L^{\mathrm{st,D}}(\Gamma))$.

The above two equations can be unified into a single one for the generalized Euler characteristic:

$$\mathcal{E}(|V_D|) = 2\delta_{0,|V_D|} + 8\pi^2 \sum_{\substack{k_n \in \Sigma(L(\Gamma)) \\ k_n \neq 0}} \frac{\sin(k_n/t)}{(k_n/t)\left((2\pi)^2 - (k_n/t)^2\right)}|_{t \geq t_0}. \tag{6}$$

Depending on the boundary conditions, $\Sigma(L(\Gamma))$ denotes either the spectrum of the Laplacian $L^{\mathrm{st}}(\Gamma)$ or $L^{\mathrm{st,D}}(\Gamma)$. In the borderline cases $|V_D| = 0$ and $|V_D| \neq 0$, $\mathcal{E}(|V_D| = 0) = \chi$ and $\mathcal{E}(|V_D| \neq 0) = \chi_G$, recovering, respectively, Equations (4) and (5).

From the experimental point of view, the usefulness of Equation (6) stems from the fact that the generalized Euler characteristic can be evaluated using only a limited number $K = K_{min}$ of the lowest eigenvalues (resonances) [21,22,68,69]

$$K \geq |V| + 2\mathcal{L}t\left[1 - \exp\left(\frac{-\epsilon\pi}{\mathcal{L}t}\right)\right]^{-1/2}, \tag{7}$$

where $|V|$ is the total number of graph vertices, $\mathcal{L} = \sum_{e \in E} l_e$ is the total length of the graph, and ϵ is the accuracy of determining the Euler characteristic from Formula (7). To obtain the smallest possible number of resonances K_{min}, for a given accuracy ϵ, we assign to t its smallest allowed value $t = t_0 = \frac{1}{2l_{min}}$. Since the Euler characteristic is an integer, the accuracy of its determination should be taken $\epsilon < 1/2$. In our calculations of K_{min}, we assumed $\epsilon = 1/4$.

2.2. A Graph Split into Two Disconnected Subgraphs

In order to simplify the description of the graphs, we introduce the following notation of graphs and networks $\Gamma(|V|, |E|, |V_D|)$, where $|V| = |V_N| + |V_D|$. A graph or network $\Gamma(|V|, |E|, |V_D|)$ contains $|V|$ vertices, including $|V_N|$ and $|V_D|$ vertices with standard (Neumann) and Dirichlet boundary conditions and $|E|$ edges.

We will consider a general situation when an original graph $\Gamma_o(|V_o|, |E_o|, |V_{D_o}|)$ is split into two disconnected subgraphs $\Gamma_i(|V_i|, |E_i|, |V_{D_i}|)$, $i = 1, 2$, at the common for the subgraphs vertices V_c, which are characterized by the Neumann boundary conditions. In the partition process, each common vertex $v \in V_c$ will be split into two new vertices belonging to the different subgraphs (see Figure 1).

The generalized Euler characteristics of the original graph and its subgraphs are $\mathcal{E}_o(|V_{D_o}|) = |V_o| - |E_o| - |V_{D_o}|$ and $\mathcal{E}_i(|V_{D_i}|) = |V_i| - |E_i| - |V_{D_i}|$, $i = 1, 2$, respectively.

The relationships between the number of vertices and edges of the graphs are the following: $|V_o| + |V_c| = |V_1| + |V_2|$, $|E_o| = |E_1| + |E_2|$. It leads to the following relationship between $\mathcal{E}_o(|V_{D_o}|)$ and $\mathcal{E}_i(|V_{D_i}|)$, $i = 1, 2$

$$\mathcal{E}_1(|V_{D_1}|) + \mathcal{E}_2(|V_{D_2}|) = \mathcal{E}_o(|V_{D_o}|) + |V_c| + |V_{D_o}| - |V_{D_1}| - |V_{D_2}|, \tag{8}$$

where $|V_c|$ denotes the number of common vertices.

In Figure 1, we show the case when the original graph $\Gamma_o(|V_o| = 6, |E_o| = 9, |V_{D_o}| = 0) = \Gamma_o(6, 9, 0)$ is divided into two subgraphs $\Gamma_1(4, 6, 0)$ and $\Gamma_2(4, 3, 0)$. Using Equation (8), one can find that the subgraphs before the disconnection were connected in $|V_c| = 2$ common vertices. In this relatively simple situation, the generalized Euler characteristics of the graphs or networks can be found from their topological properties, i.e., the numbers of vertices and edges of the graphs. However, if we do not see the graphs and therefore do not know their topological properties but we know their eigenvalues (spectra), the only available solution to the problem is to use Equation (6) to find their generalized Euler characteristics and consequently the number $|V_c|$ of the common vertices. The same situation exists for the graphs possessing the Dirichlet boundary conditions. In this case, in order to identify them, one needs to know (measure) the eigenvalues (resonances) of graphs or networks and use Equations (6) and (8) to evaluate the number $|V_c|$ of the common vertices.

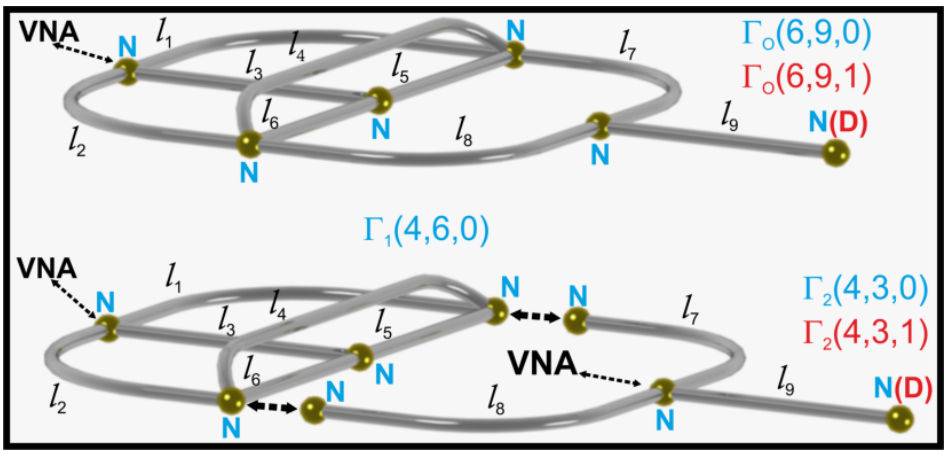

Figure 1. The scheme of the original graph $\Gamma_o(6, 9, 0)$, which was divided into two subgraphs $\Gamma_1(4, 6, 0)$ and $\Gamma_2(4, 3, 0)$. All graphs possess the vertices with the Neumann boundary conditions, which are marked by blue capital letters N. In the case of the graphs with the mixed boundary conditions, the original graph $\Gamma_o(6, 9, 1)$ was divided into two subgraphs $\Gamma_1(4, 6, 0)$ and $\Gamma_2(4, 3, 1)$. The vertices with the Dirichlet boundary conditions are marked by red capital letters D. The vertices where a vector network analyzer was connected to the microwave networks simulating quantum graphs presented in this figure are marked by VNA.

3. Measurements of the Spectra of Microwave Networks

In order to evaluate the generalized Euler characteristic $\mathcal{E}(|V_D|)$ defined by Equation (6), we measured the spectra of microwave networks simulating quantum graphs. In our investigations, we used a set-up (see Figure 2) that consisted of an Agilent E8364B vector network analyzer (VNA) and HP 85133-60016 flexible microwave cable that connected the VNA to the measured network. The flexible cable connected to the network is equivalent to attaching an infinite lead to the quantum graph [22,32]. In this way, the one-port scattering matrix $S_{11}(\nu)$ of the network was measured as a function of microwave frequency ν. The modulus of $|S_{11}(\nu)|$ was used to identify the network's resonances. In Figure 2, we also show the original microwave network $\Gamma_o(6, 9, 1)$, which possesses a single vertex with the Dirichlet boundary condition ($V_{D_o} = 1$), marked by the red capital letter D. The measured spectrum of the network $\Gamma_o(6, 9, 1)$ is shown in the inset of Figure 2 in the frequency range $\nu = [0.01, 1]$ GHz. In order to reconfirm our experimental results, the spectra of the

quantum graphs simulated by the microwave networks were also calculated numerically using the pseudo-orbits method developed in Ref. [31].

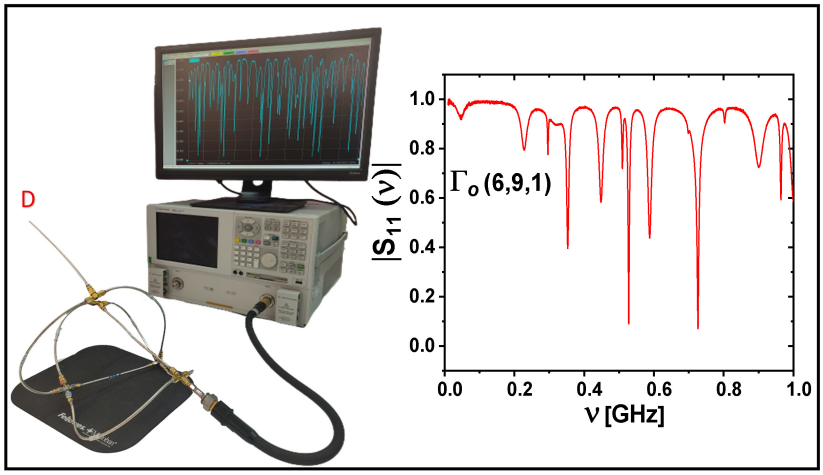

Figure 2. The experimental set-up. It contains an Agilent E8364B vector network analyzer (VNA) and HP 85133-60016 flexible microwave cable that connects the VNA to the measured network. The original microwave network $\Gamma_o(6,9,1)$ possesses a single vertex with the Dirichlet boundary condition, which is marked by the red capital letter D. The measured spectrum of the network $\Gamma_o(6,9,1)$ is shown in the inset in the frequency range $\nu = [0.01, 1]$ GHz.

In the construction of microwave networks simulating quantum graphs, we used microwave coaxial cables and junctions that corresponded to the edges and vertices of the quantum graphs. The microwave cables consisted of an outer conductor with an inner radius $r_2 = 0.15$ cm and an inner conductor of radius $r_1 = 0.05$ cm, which was surrounded by the dielectric material (Teflon). The fundamental TEM mode propagates in such cables below the cut-off frequency of the TE_{11} mode $\nu_{cut} = \frac{c}{\pi(r_1+r_2)\sqrt{\varepsilon}} = 33$ GHz [70,71], where the dielectric constant of Teflon $\varepsilon = 2.06$. It is important to point out that the lengths of edges of the simulated quantum graph have to be compared to the optical lengths of the edges of the microwave networks, i.e., $l_{opt} = \sqrt{\varepsilon} l_{ph}$, where l_{ph} is the physical length of the network edges.

In this paper, we discuss two general situations that are possible when the original network (graph) is split into two subnetworks (subgraphs): the case when the original network and its subnetworks have only the standard boundary conditions and the case when they are characterized by the mixed boundary conditions, when the Dirichlet boundary conditions are present.

3.1. Networks with the Standard Boundary Conditions

Here, we will consider the original network $\Gamma_o(|V_o|, |E_o|, |V_{D_o}|)$, which is split into two disconnected subnetworks $\Gamma_i(|V_i|, |E_i|, |V_{D_i}|)$, $i = 1, 2$, at the common for the subnetworks vertices $v \in V_c$. All networks are characterized by the standard (Neumann) boundary conditions. The experimental realizations of the networks $\Gamma_o(6,9,0)$ and its two subnetworks $\Gamma_1(4,6,0)$ and $\Gamma_2(4,3,0)$ are schematically shown in Figures 1 and 2. In this case, all networks possess only standard (Neumann) boundary conditions, denoted with the capital letter N.

The total optical lengths of the networks $\Gamma_o(6,9,0)$, $\Gamma_1(4,6,0)$, and $\Gamma_2(4,3,0)$ are $\mathcal{L}_o = 2.579$ m, $\mathcal{L}_1 = 1.675$ m, and $\mathcal{L}_2 = 0.940$ m, respectively. The lengths of their shortest edges are $l_{min_o} = l_6 = 0.221$ m, $l_{min_1} = l_6 = 0.221$ m, and $l_{min_2} = l_9 = 0.270$ m, giving $K_{min_o} = 38$, $K_{min_1} = 23$, and $K_{min_2} = 8$, respectively, which were estimated using Equation (7). Experimentally, in order to find the minimum number of resonances determined by the parameters K_{min_o}, K_{min_1}, and K_{min_2}, it was necessary to measure the spectra of the microwave networks $\Gamma_o(6,9,0)$, $\Gamma_1(4,6,0)$, and $\Gamma_2(4,3,0)$ in the frequency ranges

$[0.010, 2.347]$ GHz, $[0.010, 2.234]$ GHz, and $[0.010, 1.271]$ GHz, respectively. Taking into account the above parameters, the generalized Euler characteristics $\mathcal{E}_o(|V_{D_o}|)$, $\mathcal{E}_1(|V_{D_1}|)$, and $\mathcal{E}_2(|V_{D_2}|)$ were calculated using Equation (6).

In Figure 3a–c, we show the generalized Euler characteristics $\mathcal{E}_o(|V_{D_o}| = 0)$, $\mathcal{E}_1(|V_{D_1}| = 0)$, and $\mathcal{E}_2(|V_{D_2}| = 0)$ (red dotted lines), evaluated experimentally as a function of the parameter t. The numerically found generalized Euler characteristics are marked with blue full lines. In all three cases, for both experimental and theoretical results, the plateaus at the generalized Euler characteristics start close to the points $t_{0_o} = 2.26\ \mathrm{m}^{-1}$, $t_{0_1} = 2.26\ \mathrm{m}^{-1}$, and $t_{0_2} = 1.85\ \mathrm{m}^{-1}$ defined by the theory (see the discussion below Equation (7)). The values of the generalized Euler characteristics are found to be $\mathcal{E}_o(|V_{D_o}| = 0) = -3$, $\mathcal{E}_1(|V_{D_1}| = 0) = -2$, and $\mathcal{E}_2(|V_{D_2}| = 0) = 1$, respectively. Using Equation (8), it is easy to find that $|V_c| = 2$. It means that, before splitting, the two subgraphs were connected at the two vertices. It is important to point out that the above information was obtained without knowing anything about the topologies of the networks.

3.2. Networks with the Mixed Boundary Conditions

We used the same physical networks to investigate the split of the original network $\Gamma_o(6, 9, 1)$ possessing the mixed boundary conditions into two separated subnetworks $\Gamma_1(4, 6, 0)$ and $\Gamma_2(4, 3, 1)$. The network $\Gamma_o(6, 9, 1)$ and the subnetwork $\Gamma_2(4, 3, 1)$ possess a single Dirichlet boundary condition. Figure 1 shows the schemes of the networks. The Dirichlet boundary conditions are denoted by the capital letter D. All other parameters of the networks, such as the total lengths and the shortest edges, are the same as in the case of the networks with the standard boundary conditions, which were discussed above. However, for the networks with the mixed boundary conditions, one requires the same number of resonances as, in the case of the networks with the Neumann boundary conditions, the frequency ranges where they can be identified are different. For example, for the networks $\Gamma_o(6, 9, 1)$ and $\Gamma_2(4, 3, 1)$, they are $[0.010, 2.500]$ GHz and $[0.010, 1.131]$ GHz, respectively.

In Figure 4a–c, we show the generalized Euler characteristics $\mathcal{E}_o(|V_{D_o}| = 1)$, $\mathcal{E}_1(|V_{D_1}| = 0)$, and $\mathcal{E}_2(|V_{D_2}| = 1)$ (red dotted lines), evaluated experimentally as a function of the parameter t. The generalized Euler characteristics that were found numerically are marked with blue full lines. Moreover, here, in all three cases, for both experimental and theoretical results, the plateaus at the generalized Euler characteristics start close to the points t_{0_o}, t_{0_1}, and t_{0_2} defined by the theory. The values of the generalized Euler characteristics are found to be $\mathcal{E}_o(|V_{D_o}| = 1) = -4$, $\mathcal{E}_1(|V_{D_1}| = 0) = -2$, and $\mathcal{E}_2(|V_{D_2}| = 1) = 0$, respectively. In addition, in this case, using Equation (8), we found that $|V_c| = 2$. One should remark that in the case of the mixed boundary conditions, the knowledge of the topologies of the experimental networks does not allow us to find their generalized Euler characteristics. We also have to know the number of their Dirichlet boundary conditions. Therefore, the measurements of the spectra of the networks and using Equation (6) are mandatory.

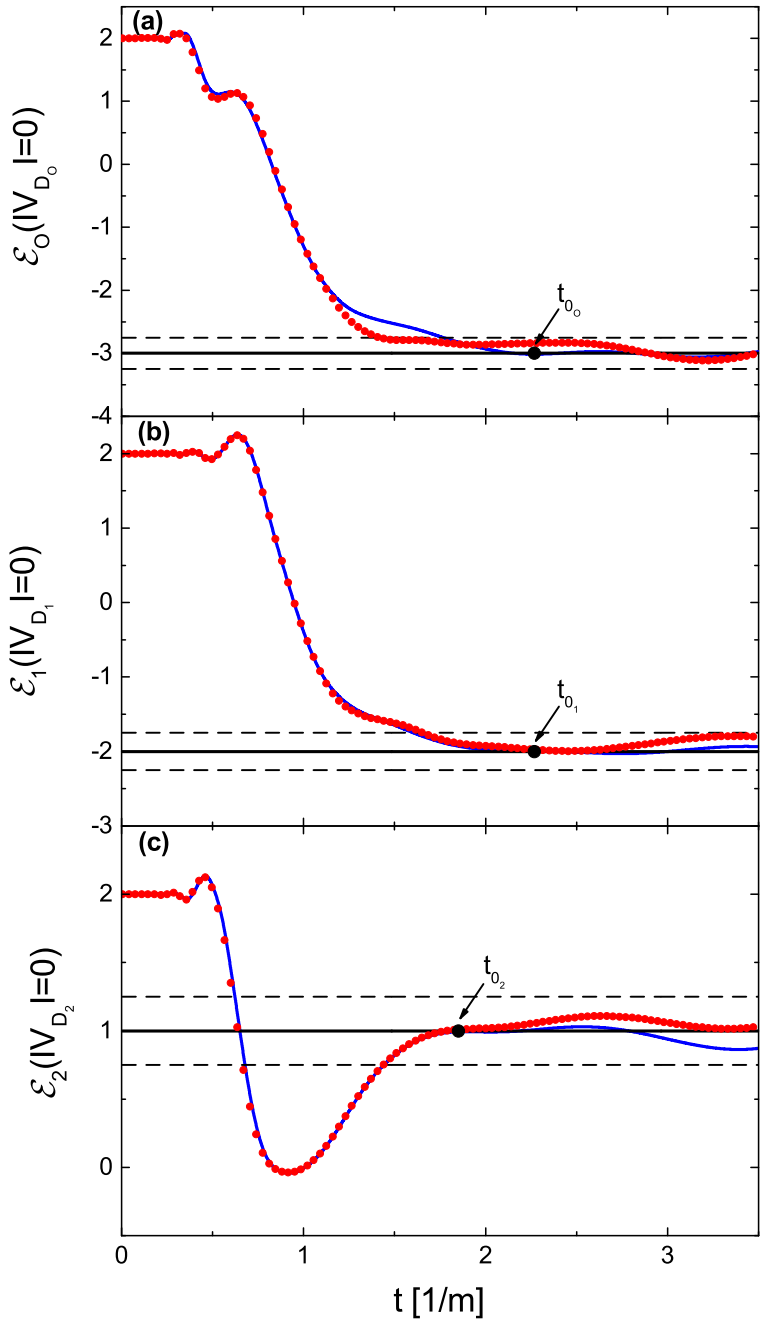

Figure 3. Generalized Euler characteristics evaluated for the networks with the standard boundary conditions as a function of the parameter t. Panels (**a**–**c**) show the generalized Euler characteristics $\mathcal{E}_o(|V_{D_o}|=0)$, $\mathcal{E}_1(|V_{D_1}|=0)$, and $\mathcal{E}_2(|V_{D_2}|=0)$ of the networks $\Gamma_o(6,9,0)$, $\Gamma_1(4,6,0)$, and $\Gamma_2(4,3,0)$, respectively. The experimental and numerical results are marked with red dotted and blue full lines, respectively. In all three cases, the plateaus at the generalized Euler characteristics start close to the points $t_{0_o}=2.26\ \mathrm{m}^{-1}$, $t_{0_1}=2.26\ \mathrm{m}^{-1}$, and $t_{0_2}=1.85\ \mathrm{m}^{-1}$, respectively, defined by the theory (see the discussion below Equation (7)). The black broken lines show the limits of the expected errors $\mathcal{E}_q(|V_{D_q}|)\pm 1/4$, where $q=o,1,$ and 2.

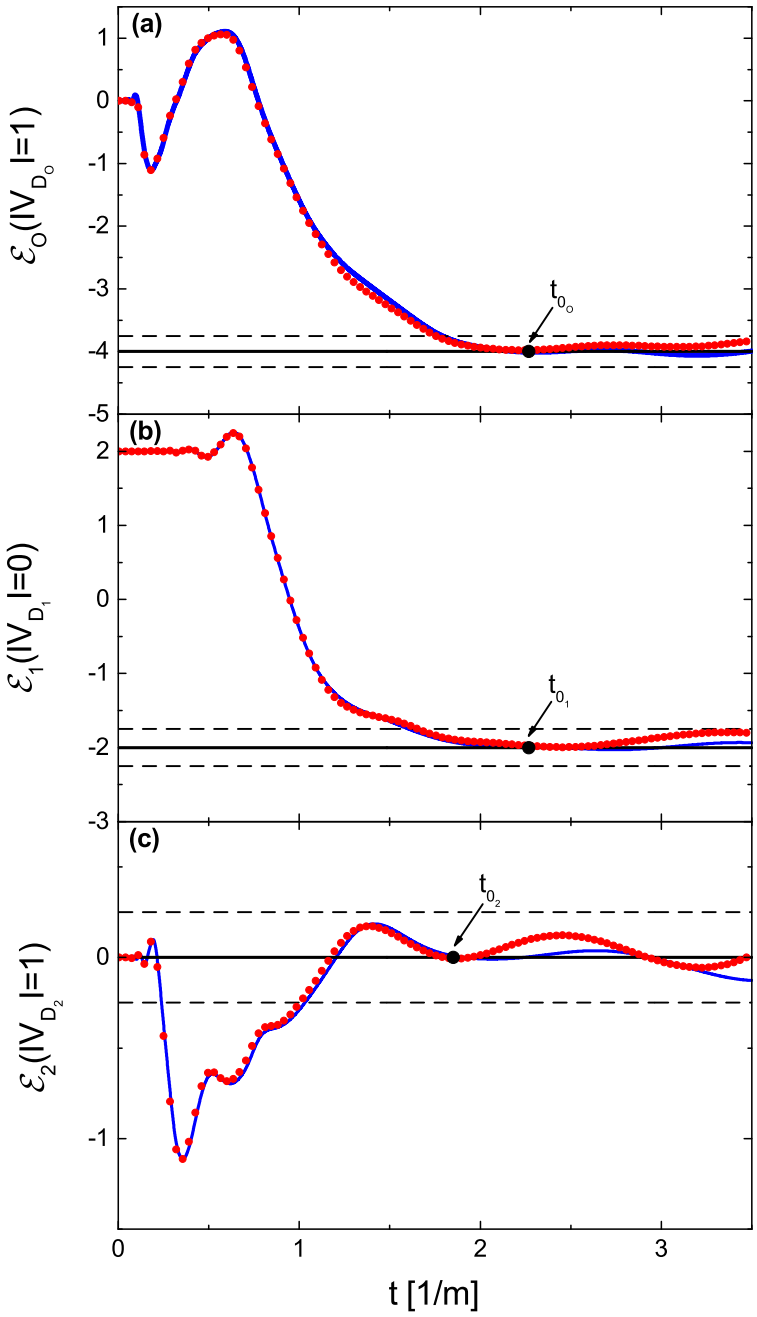

Figure 4. Generalized Euler characteristics evaluated for the networks with the mixed boundary conditions as a function of the parameter t. Panels (**a**–**c**) show the generalized Euler characteristics $\mathcal{E}_o(|V_{D_o}|=1)$, $\mathcal{E}_1(|V_{D_1}|=0)$, and $\mathcal{E}_2(|V_{D_2}|=1)$ of the networks $\Gamma_o(6,9,1)$, $\Gamma_1(4,6,0)$, and $\Gamma_2(4,3,1)$, respectively. The experimental and numerical results are marked with red dotted and blue full lines, respectively. Moreover, here, in all three cases, the plateaus at the generalized Euler characteristics start close to the points $t_{0_o}=2.26\ \mathrm{m}^{-1}$, $t_{0_1}=2.26\ \mathrm{m}^{-1}$, and $t_{0_2}=1.85\ \mathrm{m}^{-1}$, respectively, defined by the theory. The black broken lines show the limits of the expected errors $\mathcal{E}_q(|V_{D_q}|)\pm 1/4$, where $q=o,1,$ and 2.

4. Summary

We analyzed a relationship between the generalized Euler characteristic $\mathcal{E}_o(|V_{D_o}|)$ of the original graph (network), which was split into two disconnected subgraphs (subnetworks) $i=1,2$, and their generalized Euler characteristics $\mathcal{E}_i(|V_{D_i}|)$. We showed that the evaluation of the generalized Euler characteristics $\mathcal{E}_o(|V_{D_o}|)$ and $\mathcal{E}_i(|V_{D_i}|)$ allows us

to determine the number $|V_c|$ of common vertices where the two subgraphs were initially connected. The theoretical results were numerically verified and confirmed experimentally using microwave networks with the standard and mixed boundary conditions. The application of the generalized Euler characteristics defined by Equation (6) requires the measurement of the spectra of the networks but in return allows us to find $|V_c|$ without knowing their topologies. Therefore, it might be possible to apply the properties of the splitting networks discussed in this article in some more practical applications, such as the diagnostics of electronic or microwave networks. One should underline that the first practical test of such diagnostics where the properties of splitting networks and the generalized Euler characteristic were applied was presented in this article. For this purpose, we used real-world systems, such as microwave networks. They are open and dissipative systems, which are completely different from the ideal dissipationless graphs considered in their mathematical studies. In spite of this, even for more complex networks possessing the mixed boundary conditions, we were able to find experimentally the number of common vertices $|V_c|$ where the two separated subnetworks were connected before their splitting.

Author Contributions: O.F. performed the experiment. M.Ł. performed numerical calculations. O.F., M.Ł., A.A. and S.B. performed the data analysis. L.S. provided the theoretical interpretation. L.S. wrote the manuscript. All authors have read and agreed to the published version of the manuscript.

Funding: This research study was funded by the National Science Centre, Poland, Grant No. 2018/30/Q/ ST2/00324.

Institutional Review Board Statement: Not applicable.

Informed Consent Statement: Not applicable.

Data Availability Statement: The data that support the results presented in this paper and other findings of this study are available from the corresponding authors upon reasonable request.

Conflicts of Interest: The authors declare no conflict of interest.

References

1. Euler, L. Solutio problematis ad geometriam situs pertinentis. *Comment. Acad. Sci. Imp. Petropol.* **1736**, *8*, 128–140.
2. Pauling, L. The diamagnetic anisotropy of aromatic molecules. *J. Chem. Phys.* **1936**, *4*, 673–677. [CrossRef]
3. Sánchez-Gil, J.A.; Freilikher, V.; Yurkevich, I.; Maradudin, A.A. Coexistence of ballistic transport, diffusion, and localization in surface disordered waveguides. *Phys. Rev. Lett.* **1998**, *80*, 948–953. [CrossRef]
4. Kowal, D.; Sivan, U.; Entin-Wohlman, O.; Imry, Y. Transmission through multiply-connected wire systems. *Phys. Rev. B* **1990**, *42*, 9009–9018. [CrossRef] [PubMed]
5. Imry, Y. *Introduction to Mesoscopic Physics*; Oxford University Press: New York, NY, USA, 1997; p. 234.
6. Hu, W.; Pillay, J.C.; Wu, K.; Pasek, M.; Shum, P.P.; Chong, Y.D. Measurement of a topological edge invariant in a microwave network. *Phys. Rev. X* **2015**, *5*, 011012. [CrossRef]
7. Szameit, A. Photonics: Chaos from symmetry. *Nat. Phys.* **2015**, *11*, 895–896. [CrossRef]
8. Exner, P.; Šeba, P.; Stovicek, P. Quantum interference on graphs controlled by an external electric field. *J. Phys. A Math. Gen.* **1988**, *21*, 4009–4019. [CrossRef]
9. Kottos, T.; Smilansky, U. Quantum chaos on graphs. *Phys. Rev. Lett.* **1997**, *79*, 4794–4797. [CrossRef]
10. Kottos, T.; Smilansky, U. Periodic Orbit Theory and Spectral Statistics for Quantum Graphs. *Ann. Phys.* **1999**, *274*, 76–124. [CrossRef]
11. Blümel, R.; Dabaghian, Y.; Jensen, R.V. Explicitly Solvable Cases of One-Dimensional Quantum Chaos. *Phys. Rev. Lett.* **2002**, *88*, 4. [CrossRef]
12. Berkolaiko, G.; Kuchment, P. Introduction to Quantum Graphs. In *Mathematical Surveys and Monographs*; American Mathematical Society, Providence, RI, USA, 2013; p. 270.
13. Pluhar, Z.; Weidenmueller, H.A. Universal Quantum Graphs. *Phys. Rev. Lett.* **2014**, *112*, 144102. [CrossRef] [PubMed]
14. Pinheiro, L.K.; Souza, B.S.; Trevisan, V. Determining Graphs by the Complementary Spectrum. *Discuss. Math.—Graph Theory* **2020**, *40*, 607–620. [CrossRef]
15. Białous, M.; Dulian, P.; Sawicki, A.; Sirko, L. Delay-time distribution in the scattering of short Gaussian pulses in microwave networks. *Phys. Rev. E* **2021**, *104*, 024223. [CrossRef] [PubMed]
16. Hul, O.; Ławniczak, M.; Bauch, S.; Sawicki, A.; Kuś, M.; Sirko, L. Are scattering properties of graphs uniquely connected to their shapes? *Phys. Rev. Lett.* **2012**, *109*, 040402. [CrossRef]

17. Gadomski, A.; Łuczka, J.; Rudnicki, R. Finite volume effects in a model grain growth. *Phys. A Stat. Mech. Appl.* **2003**, *325*, 284–291. [CrossRef]
18. Gadomski, A.; Kruszewska, N. On clean grain-boundaries involving growth of nonequilibrium crystalline-amorphous superconducting materials addressed by a phenomenological viewpoint. *Eur. Phys. J. B* **2012**, *85*, 1–8. [CrossRef]
19. Kurasov, P. Graph Laplacians and topology. *Ark. Mat.* **2008**, *46*, 95–111. [CrossRef]
20. Kurasov, P. Schrödinger operators on graphs and geometry I: Essentially bounded potentials. *J. Funct. Anal.* **2008**, *254*, 934–953. [CrossRef]
21. Ławniczak, M.; Kurasov, P.; Bauch, S.; Białous, M.; Yunko, V.; Sirko, L. Hearing Euler characteristic of graphs. *Phys. Rev. E* **2020**, *101*, 052320. [CrossRef]
22. Ławniczak, M.; Kurasov, P.; Bauch, S.; Białous, M.; Akhshani, A.; Sirko, L. A new spectral invariant for quantum graphs. *Sci. Rep.* **2021**, *11*, 15342. [CrossRef]
23. Bauch, S.; Ławniczak, M.; Wrochna, J.; Kurasov, P.; Sirko, L. Some Applications of Generalized Euler Characteristic of Quantum Graphs and Microwave Networks. *Acta Phys. Pol. A* **2021**, *140*, 525–531. [CrossRef]
24. Hul, O.; Bauch, S.; Pakoński, P.; Savytskyy, N.; Życzkowski, K.; Sirko, L. Experimental simulation of quantum graphs by microwave networks. *Phys. Rev. E* **2004**, *69*, 7. [CrossRef] [PubMed]
25. Ławniczak, M.; Hul, O.; Bauch, S.; Šeba, P.; Sirko, L. Experimental and numerical investigation of the reflection coefficient and the distributions of Wigner's reaction matrix for irregular graphs with absorption. *Phys. Rev. E* **2008**, *77*, 056210. [CrossRef] [PubMed]
26. Ławniczak, M.; Bauch, S.; Sirko, L. Application of Microwave Networks to Simulation of Quantum Graphs. In *Handbook of Applications of Chaos Theory*; Chapman and Hall/CRC: New York, NY, USA, 2016; pp. 559–584.
27. Dietz, B.; Yunko, V.; Białous, M.; Bauch, S.; Ławniczak, M.; Sirko, L. Nonuniversality in the spectral properties of time-reversal-invariant microwave networks and quantum graphs. *Phys. Rev. E* **2017**, *95*, 052202. [CrossRef] [PubMed]
28. Ławniczak, M.; Sirko, L. Investigation of the diagonal elements of the Wigner's reaction matrix for networks with violated time reversal invariance. *Sci. Rep.* **2019**, *9*, 5630. [CrossRef] [PubMed]
29. Yunko, V.; Białous, M.; Sirko, L. Edge switch transformation in microwave networks. *Phys. Rev. E* **2020**, *102*, 012210. [CrossRef]
30. Hul, O.; Tymoshchuk, O.; Bauch, S.; Koch, P.M.; Sirko, L. Experimental investigation of Wigner's reaction matrix for irregular graphs with absorption. *J. Phys. A Math. Theor.* **2005**, *38*, 10489. [CrossRef]
31. Lipovský, J. On the effective size of a non-Weyl graph. *J. Phys. A Math. Theor* **2016**, *49*, 375202. [CrossRef]
32. Ławniczak, M.; Lipovský, J.; Sirko, L. Non-Weyl microwave graphs. *Phys. Rev. Lett.* **2019**, *122*, 140503. [CrossRef]
33. Ławniczak, M.; Bauch, S.; Hul, O.; Sirko, L. Experimental investigation of the enhancement factor for microwave irregular networks with preserved and broken time reversal symmetry in the presence of absorption. *Phys. Rev. E* **2010**, *81*, 046204. [CrossRef]
34. Allgaier, M.; Gehler, S.; Barkhofen, S.; Stöckmann, H.J.; Kuhl, U. Spectral properties of microwave graphs with local absorption. *Phys. Rev. E* **2014**, *89*, 022925. [CrossRef] [PubMed]
35. Białous, M.; Yunko, V.; Bauch, S.; Ławniczak, M.; Dietz, B.; Sirko, L. Power Spectrum Analysis and Missing Level Statistics of Microwave Graphs with Violated Time Reversal Invariance. *Phys. Rev. Lett.* **2016**, *117*, 144101. [CrossRef] [PubMed]
36. Ławniczak, M.; Białous, M.; Yunko, V.; Bauch, S.; Dietz, B.; Sirko, L. Analysis of missing level statistics for microwave networks simulating quantum chaotic graphs without time reversal symmetry—The case of randomly lost resonances. *Acta Phys. Pol. A* **2017**, *132*, 1672–1676. [CrossRef]
37. Rehemanjiang, A.; Allgaier, M.; Joyner, C.H.; Müller, S.; Sieber, M.; Kuhl, U.; Stöckmann, H.J. Microwave Realization of the Gaussian Symplectic Ensemble. *Phys. Rev. Lett.* **2016**, *117*, 064101. [CrossRef] [PubMed]
38. Dietz, B.; Friedrich, T.; Harney, H.L.; Miski-Oglu, M.; Richter, A.; Schäfer, F.; Weidenmüller, H.A. Quantum chaotic scattering in microwave resonators. *Phys. Rev. E* **2010**, *81*, 036205. [CrossRef]
39. Yeh, J.H.; Drikas, Z.; Gil Gil, J.; Hong, S.; Taddese, B.; Ott, E.; Antonsen, T.; Andreadis, T.; Anlage, S. Impedance and Scattering Variance Ratios of Complicated Wave Scattering Systems in the Low Loss Regime. *Acta Phys. Pol. A* **2013**, *124*, 1045–1052. [CrossRef]
40. Zheng, X.; Hemmady, S.; Antonsen, T.M.; Anlage, S.M.; Ott, E. Characterization of fluctuations of impedance and scattering matrices in wave chaotic scattering. *Phys. Rev. E* **2006**, *73*, 046208. [CrossRef]
41. Stöckmann, H.J.; Stein, J. "Quantum" chaos in billiards studied by microwave absorption. *Phys. Rev. Lett.* **1990**, *64*, 2215–2218. [CrossRef]
42. Sridhar, S.; Kudrolli, A. Experiments on not "hearing the shape" of drums. *Phys. Rev. Lett.* **1994**, *72*, 2175–2178. [CrossRef]
43. Sirko, L.; Koch, P.M.; Blümel, R. Experimental Identification of Non-Newtonian Orbits Produced by Ray Splitting in a Dielectric-Loaded Microwave Cavity. *Phys. Rev. Lett.* **1997**, *78*, 2940–2943. [CrossRef]
44. Hlushchuk, Y.; Kohler, A.; Bauch, S.; Sirko, L.; Blümel, R.; Barth, M.; Stöckmann, H.J. Autocorrelation function of level velocities for ray-splitting billiards. *Phys. Rev. E* **2000**, *61*, 366–370. [CrossRef] [PubMed]
45. Hlushchuk, Y.; Błedowski, A.; Savytskyy, N.; Sirko, L. Numerical Investigation of Regimes of Wigner and Shnirelman Ergodicity in Rough Billiards. *Phys. Scr.* **2001**, *64*, 192–196. [CrossRef]
46. Hlushchuk, Y.; Sirko, L.; Kuhl, U.; Barth, M.; Stöckmann, H.J. Experimental investigation of a regime of Wigner ergodicity in microwave rough billiards. *Phys. Rev. E* **2001**, *63*, 046208. [CrossRef]

47. Blümel, R.; Koch, P.M.; Sirko, L. Ray-Splitting Billiards. *Foun. Phys.* **2001**, *31*, 269–281. [CrossRef]
48. Dhar, A.; Madhusudhana Rao, D.; Shankar, U.; Sridhar, S. Isospectrality in chaotic billiards. *Phys. Rev. E* **2003**, *68*, 5. [CrossRef] [PubMed]
49. Savytskyy, N.; Hul, O.; Sirko, L. Experimental investigation of nodal domains in the chaotic microwave rough billiard. *Phys. Rev. E* **2004**, *70*, 6. [CrossRef]
50. Hemmady, S.; Zheng, X.; Ott, E.; Antonsen, T.M.; Anlage, S.M. Universal impedance fluctuations in wave chaotic systems. *Phys. Rev. Lett.* **2005**, *94*, 014102. [CrossRef]
51. Hul, O.; Savytskyy, N.; Tymoshchuk, O.; Bauch, S.; Sirko, L. Investigation of nodal domains in the chaotic microwave ray-splitting rough billiard. *Phys. Rev. E* **2005**, *72*, 066212. [CrossRef]
52. Dietz, B.; Richter, A. Quantum and wave dynamical chaos in superconducting microwave billiards. *Chaos* **2015**, *25*, 97601. [CrossRef]
53. Białous, M.; Dietz, B.; Sirko, L. Experimental investigation of the elastic enhancement factor in a microwave cavity emulating a chaotic scattering system with varying openness. *Phys. Rev. E* **2019**, *100*, 012210. [CrossRef]
54. Dietz, B.; Klaus, T.; Miski-Oglu, M.; Richter, A.; Wunderle, M. Partial time-reversal invariance violation in a flat, superconducting microwave cavity with the shape of a chaotic Africa billiard. *Phys. Rev. Lett.* **2019**, *123*, 174101. [CrossRef] [PubMed]
55. Blümel, R.; Buchleitner, A.; Graham, R.; Sirko, L.; Smilansky, U.; Walther, H. Dynamical localization in the microwave interaction of Rydberg atoms: The influence of noise. *Phys. Rev. A* **1991**, *44*, 4521. [CrossRef] [PubMed]
56. Jensen, R.V.; Susskind, S.M.; Sanders, M.M. Chaotic ionization of highly excited hydrogen atoms: Comparison of classical and quantum theory with experiment. *Phys. Rep.* **1991**, *201*, 1–56. [CrossRef]
57. Bellermann, M.; Bergeman, T.; Haffmans, A.; Koch, P.M.; Sirko, L. Electric-field dependence of E1 transitions between highly excited hydrogen Stark sublevels. *Phys. Rev. A* **1992**, *46*, 5836. [CrossRef] [PubMed]
58. Sirko, L.; Yoakum, S.; Haffmans, A.; Koch, P.M. Microwave-driven He Rydberg atoms: Floquet-state degeneracy lifted by a second frequency, Stueckelberg oscillations, and their destruction by added noise. *Phys. Rev. A* **1993**, *47*, R782. [CrossRef]
59. Buchleitner, A.; Delande, D. Quantum dynamics of a circular Rydberg state in a microwave field. *Phys. Rev. Lett.* **1993**, *71*, 3633. [CrossRef]
60. Sirko, L.; Bellermann, M.R.; Haffmans, A.; Koch, P.M.; Richards, D. Probing quantal dynamics of mixed phase space systems with noise. *Phys. Rev. Lett.* **1993**, *71*, 2895. [CrossRef]
61. Bayfield, J.E.; Luie, S.Y.; Perotti, L.C.; Skrzypkowski, M.P. Excited hydrogen atoms in pulsed microwaves: Journeys to quantum chaos and back. *Physics D* **1995**, *83*, 46–54. [CrossRef]
62. Sirko, L.; Koch, P. The pendulum approximation for the main quantal resonance zone in periodically driven hydrogen atoms. *Appl. Phys. B* **1995**, *60*, S195.
63. Sirko, L.; Haffmans, A.; Bellermann, M.R.; Koch, P.M. Microwave "ionization" of excited hydrogen atoms: Frequency dependence in a resonance zone. *Eur. Lett.* **1996**, *33*, 181. [CrossRef]
64. Kaulakys, B.; Ciziunas, A. A theoretical determination of the diffusion-like ionisation time of Rydberg atoms. *J. Phys. B Atom. Mol. Phys.* **1987**, *20*, 1031. [CrossRef]
65. Sirko, L.; Zelazny, S.A.; Koch, P.M. Use of the relative phase in a bichromatic field pulse to control a quasienergy gap. *Phys. Rev. Lett.* **2001**, *87*, 43002-1–43002-4. [CrossRef] [PubMed]
66. Sirko, L.; Koch, P.M. Control of common resonances in bichromatically driven hydrogen atoms. *Phys. Rev. Lett.* **2002**, *89*, 274101. [CrossRef] [PubMed]
67. Arakelyan, A.; Nunkaew, J.; Gallagher, T.F. Ionization of Na Rydberg atoms by a 79-GHz microwave field. *Phys. Rev. A* **2016**, *94*, 053416. [CrossRef]
68. Ławniczak, M.; Kurasov, P.; Bauch, S.; Białous, M.; Sirko, L. The Relationship Between the Euler Characteristic and the Spectra of Graphs and Networks. In Proceedings of the Chaotic Modeling and Simulation International Conference, Florence, Italy, 9–12 June 2020; pp. 487–497.
69. Ławniczak, M.; Kurasov, P.; Bauch, S.; Białous, M.; Sirko, L. Euler characteristic of graphs and networks. *Acta Phys. Pol. A* **2021**, *139*, 323–327. [CrossRef]
70. Jones, D.S. *The Theory of Electromagnetism*; Pergamon Press: Oxford, UK, 1964.
71. Savytskyy, N.; Kohler, A.; Bauch, S.; Blümel, R.; Sirko, L. Parametric correlations of the energy levels of ray-splitting billiards. *Phys. Rev. E* **2001**, *64*, 5. [CrossRef]